## 5.4.3 Electrical Characteristics of Large Dimension Poly-Si Thin Film Transistors with a-Si Spacer Structure

### 5.4.3.1 a-Si Spacer with a Thickness of 1500Å

In the proposed crystallization technique, owing to the tiny width of the a-Si spacer (< 1000Å), the a-Si spacers can be arrange periodically inside the channel region. Consequently, periodic lateral grain growth can be fabricated at the channel region for large-dimension device. Figure 5.22(a) ~ 5.22(f) show the typical transfer characteristics of poly-Si TFTs crystallized using 1500Å-thick a-Si spacer structure with channel length of 10 μm, in which the distances between neighboring a-Si spacers are 1 μm, 1.5 μm, 2 μm, 2.5 μm, 3 μm, and 4 μm, respectively. The laser process conditions are optimized. Several important electrical characteristics of the TFTs are summarized in Table 5.3. For comparison, the conventional ELC poly-Si TFTs with a thickness of 1000Å were also fabricated. To obtain high-performance LTPS TFTs, a laser shot density per area of 100 and substrate temperature of 400°C were used for the fabrication of conventional ELC poly-Si TFTs. The laser fluence was also controlled in SLG regime to obtain a large-grain poly-Si thin film. The periodic large longitudinal grains in the channel region make the performance of ELC poly-Si with a-Si spacer structure much better than that of the conventional counterparts, especially for the improvement of field-effect mobility. Besides, high on/off current ratio ($>10^7$) and low threshold voltage are also exhibited in these devices. These electrical characteristics are continuous to improve gradually owing to the decrease of grain boundary in the channel region as the distance between the adjacent a-Si spacers increase. The best electrical characteristics are obtained when the distance between the neighboring a-Si spacers is 2.5 μm. This is consisting with the previous SEM analysis results, which reveal the largest longitudinal grain in this crystallization technique is about 2.5 μm. Although fine and small grains are existed in the channel region as the distance between neighboring a-Si spacers exceeds 2.5 μm, the performance of ELC poly-Si TFT with a-Si spacer structure is still superior to that of the conventional ELC poly-Si TFT. This can be also attributed to the large longitudinal grains occurring in the channel region.

**Table 5.3.** Measured optimal electrical characteristics of TFTs crystallized with conventional and a-Si spacer structure, in which the distances between neighboring a-Si spacers are 1 μm, 1.5 μm, 2 μm, 2.5 μm, 3 μm, and 4 μm, respectively. The device channel length and width are 10μm. The a-Si spacer thickness is 1500Å.

| Structure | Threshold Voltage (V) | Mobility ($cm^2$/V-s) | Subthreshold Swing (V/dec) | $I_{on}/I_{off}$ @ $V_{ds}$ = -5V |
|---|---|---|---|---|
| Conventional TFT | 6.16 | 113 | 1.61 | $9.27x10^6$ |
| a-Si-spacer TFT<br>spacer distance = 1μm | 5.88 | 140 | 1.68 | $2.49x10^7$ |
| a-Si-spacer TFT<br>spacer distance = 1.5μm | 5.44 | 147 | 1.64 | $2.39x10^7$ |
| a-Si-spacer TFT<br>spacer distance = 2μm | 5.66 | 167 | 1.71 | $1.01x10^7$ |
| a-Si-spacer TFT<br>spacer distance = 2.5μm | 5.68 | 191 | 1.52 | $1.43x10^7$ |
| a-Si-spacer TFT<br>spacer distance = 3μm | 5.49 | 170 | 1.61 | $3.82x10^7$ |
| a-Si-spacer TFT<br>spacer distance = 4μm | 5.64 | 166 | 1.67 | $4.27x10^7$ |

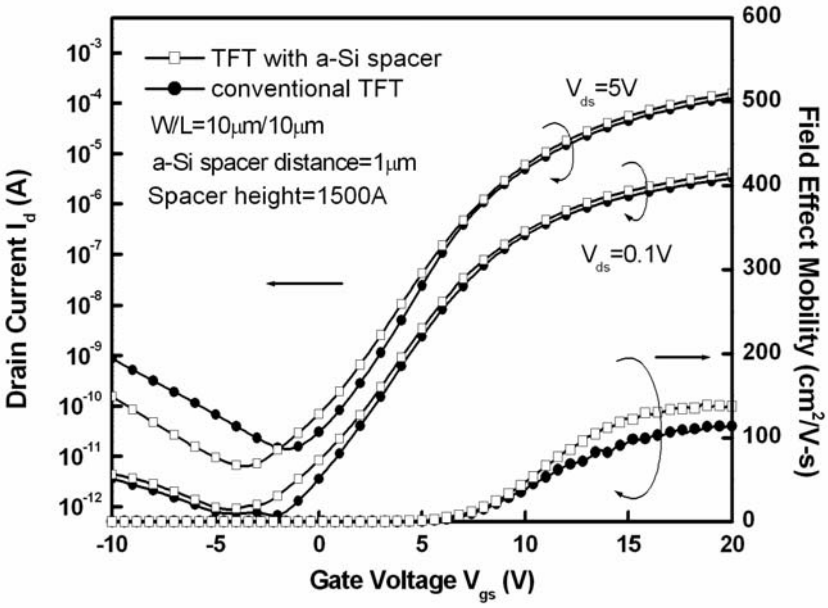

Figure 5.22(a). The typical transfer characteristics of poly-Si TFTs crystallized using 1500Å-thick a-Si spacer structure with channel length of 10 μm, in which the distance between neighboring a-Si spacers is 1 μm.

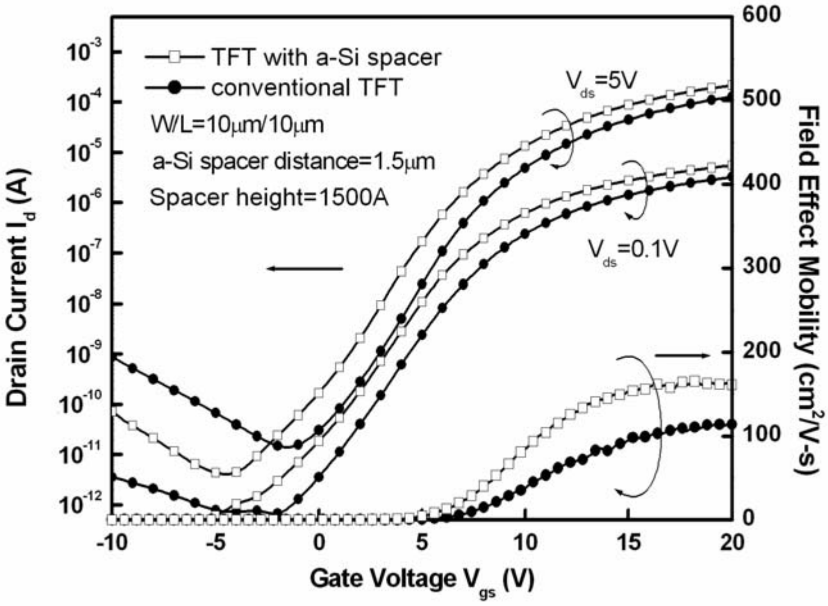

Figure 5.22(b). The typical transfer characteristics of poly-Si TFTs crystallized using 1500Å-thick a-Si spacer structure with channel length of 10 μm, in which the distance between neighboring a-Si spacers is 1.5 μm.

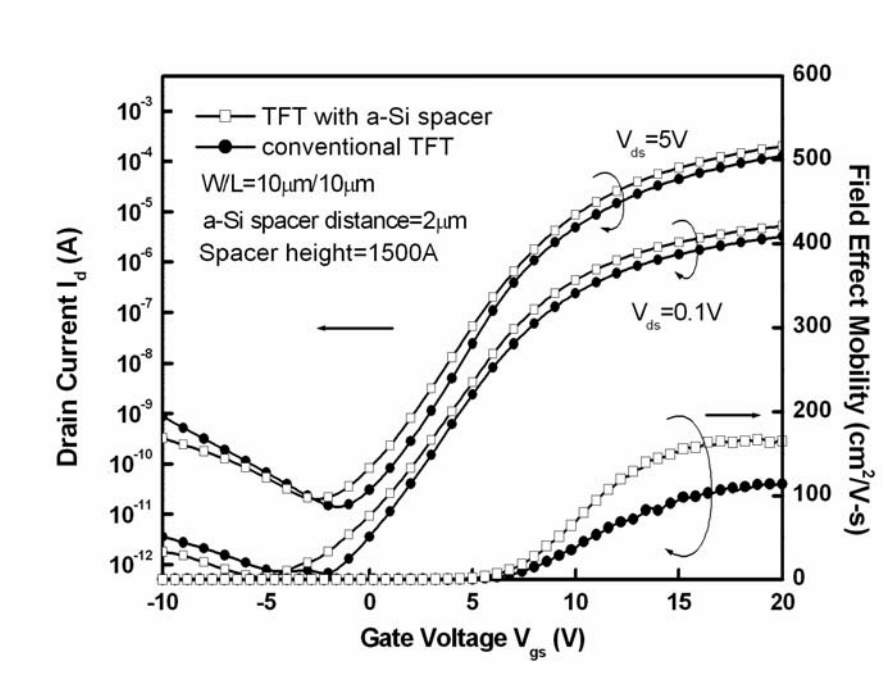

Figure 5.22(c). The typical transfer characteristics of poly-Si TFTs crystallized using 1500Å-thick a-Si spacer structure with channel length of 10 μm, in which the distance between neighboring a-Si spacers is 2 μm.

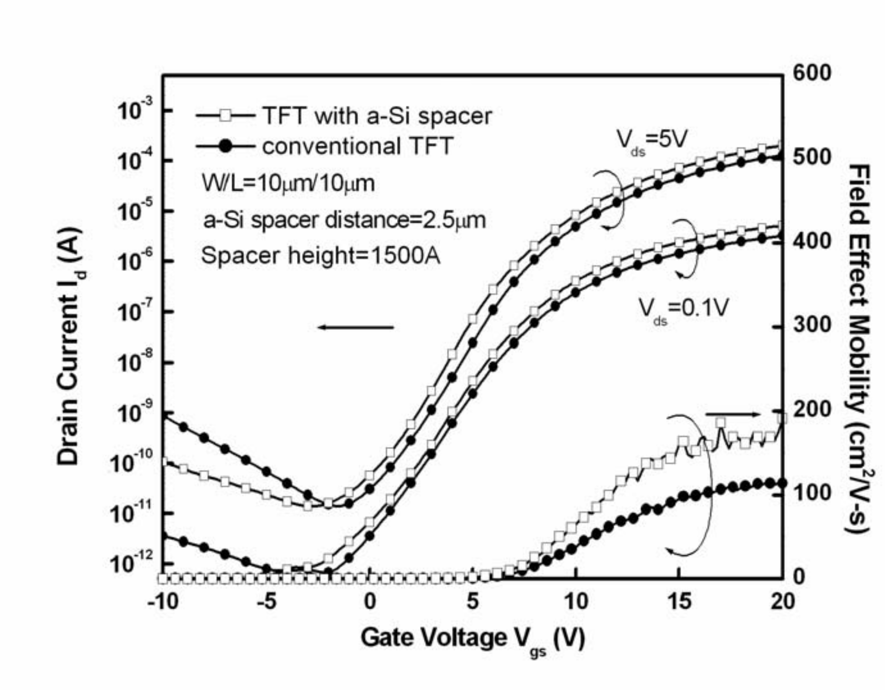

Figure 5.22(d). The typical transfer characteristics of poly-Si TFTs crystallized using 1500Å-thick a-Si spacer structure with channel length of 10 μm, in which the distance between neighboring a-Si spacers is 2.5 μm.

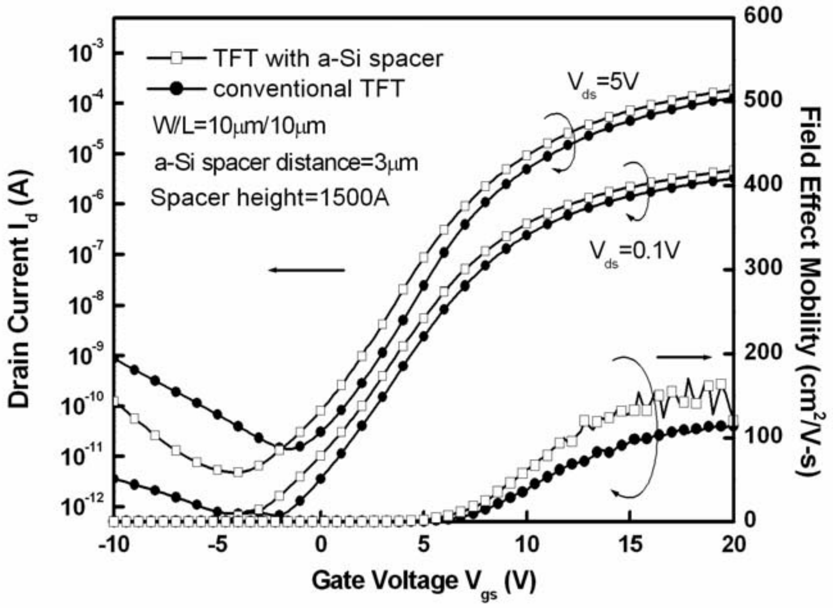

Figure 5.22(e). The typical transfer characteristics of poly-Si TFTs crystallized using 1500Å-thick a-Si spacer structure with channel length of 10 μm, in which the distance between neighboring a-Si spacers is 3 μm.

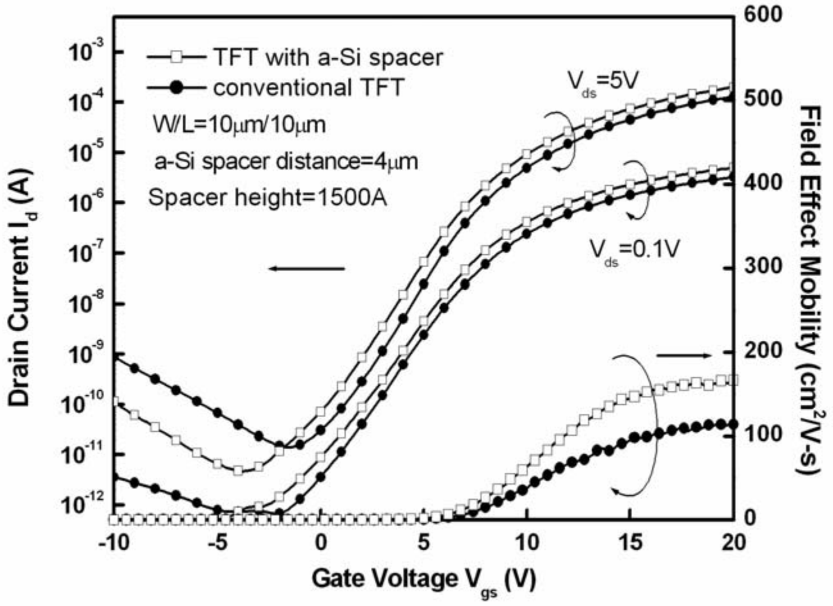

Figure 5.22(f). The typical transfer characteristics of poly-Si TFTs crystallized using 1500Å-thick a-Si spacer structure with channel length of 10 μm, in which the distance between neighboring a-Si spacers is 4 μm.

Figure 5.23(a) ~ Figure 5.23(f) show the output characteristics of ELC poly-Si TFTs crystallized using 1500Å-thick a-Si spacer structure with channel length of 10 μm, in which the distances between neighboring a-Si spacers are 1 μm, 1.5 μm, 2 μm, 2.5 μm, 3 μm, and 4 μm, respectively. In order to avoid the threshold voltage difference, the applied gate driving voltages are kept at constant values of |Vg-Vth| = 12V and 16V, respectively. Owing to the high field effect mobility, the poly-Si TFTs with a-Si spacer structure exhibit high driving current than the conventional ELC poly-S TFTs. In addition, the self-heating effect is not observed in these large dimension devices. One possible reason is the lower drain current compared with that of small dimension devices. The other reason may be attributed to the large thermal dispassion area as the channel width area increases.

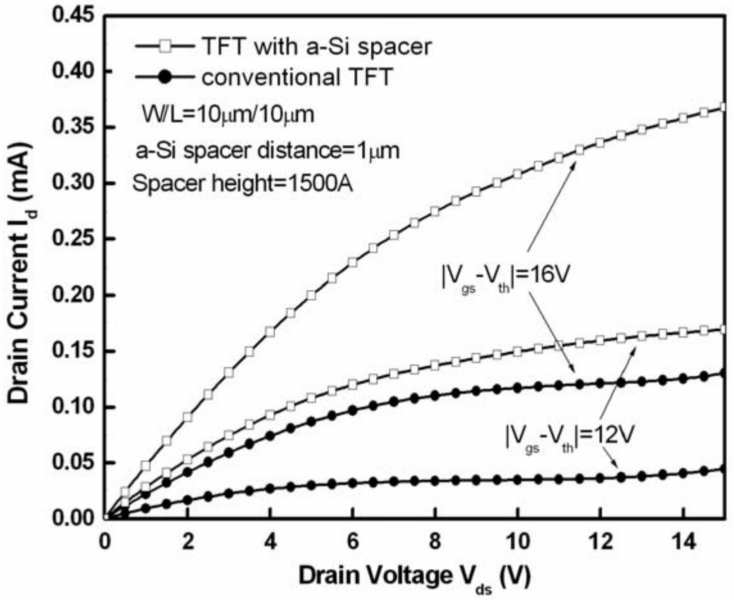

Figure 5.23(a). The output characteristics of ELC poly-Si TFTs crystallized using 1500Å-thick a-Si spacer structure with channel length of 10 μm, in which the distance between neighboring a-Si spacers is 1 μm.

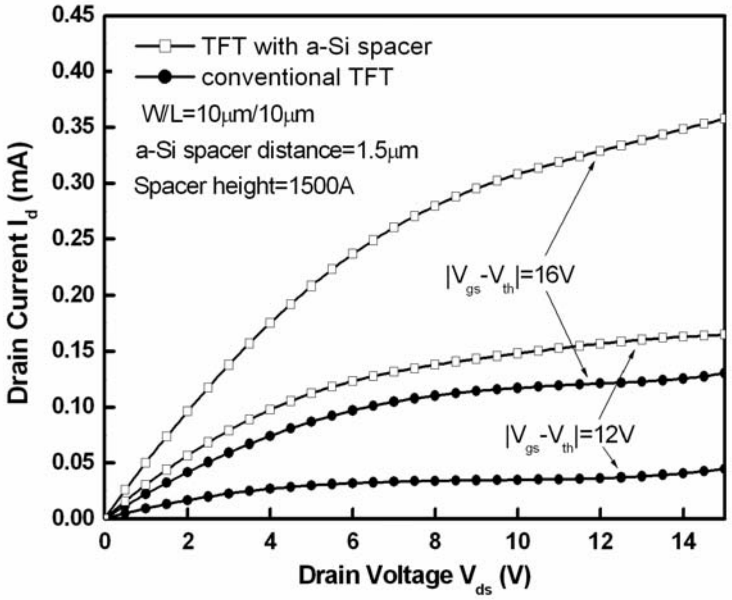

Figure 5.23(b). The output characteristics of ELC poly-Si TFTs crystallized using 1500Å-thick a-Si spacer structure with channel length of 10 μm, in which the distance between neighboring a-Si spacers is 1.5 μm.

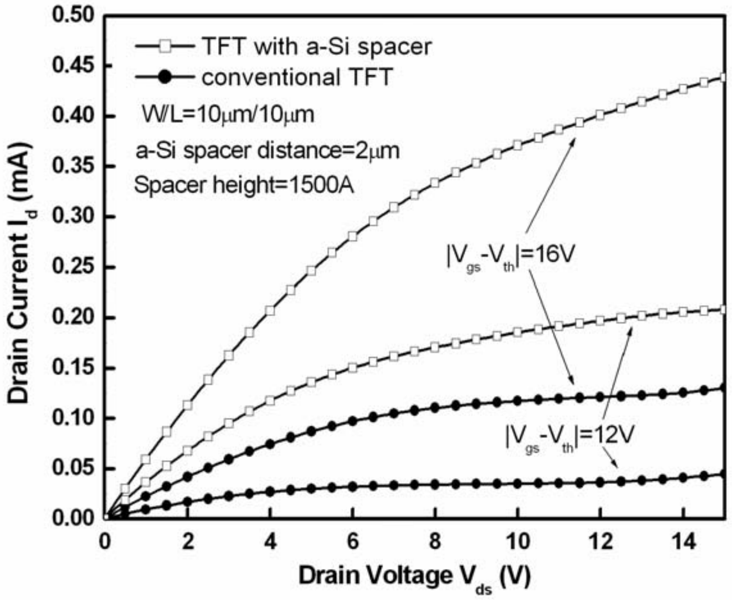

Figure 5.23(c). The output characteristics of ELC poly-Si TFTs crystallized using 1500Å-thick a-Si spacer structure with channel length of 10 μm, in which the distance between neighboring a-Si spacers is 2 μm.

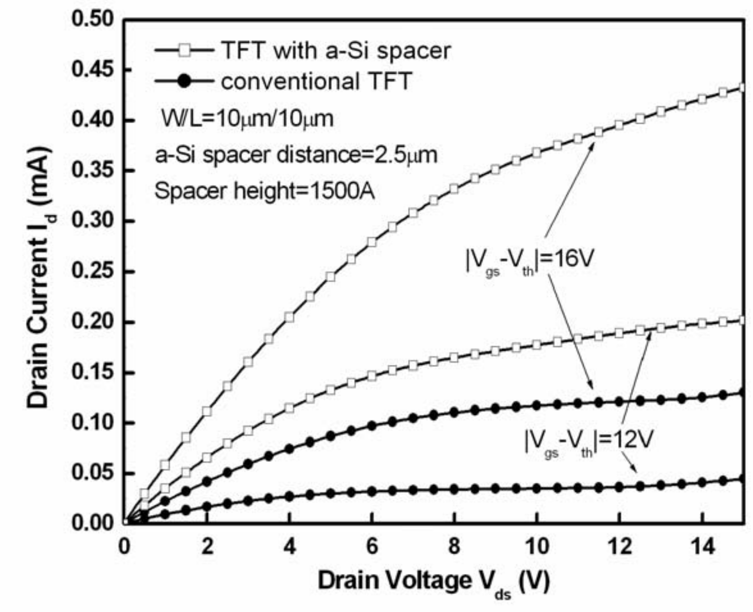

Figure 5.23(d). The output characteristics of ELC poly-Si TFTs crystallized using 1500Å-thick a-Si spacer structure with channel length of 10 μm, in which the distance between neighboring a-Si spacers is 2.5 μm.

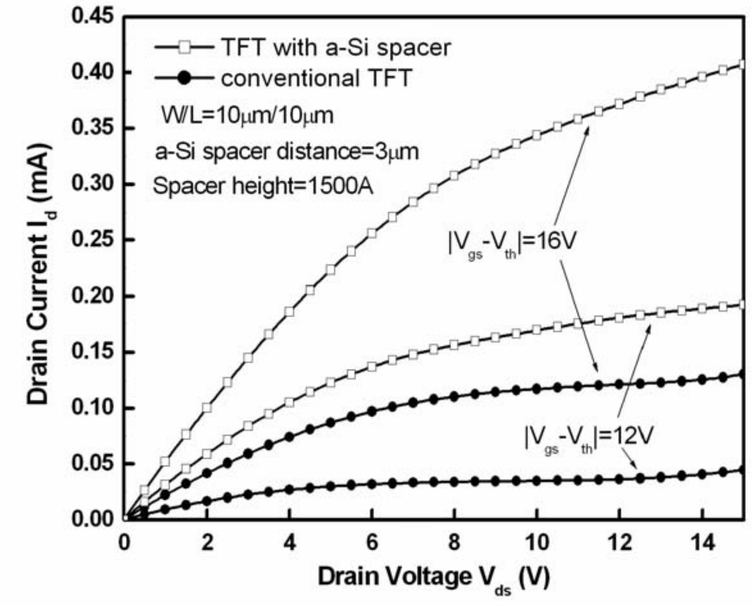

Figure 5.23(e). The output characteristics of ELC poly-Si TFTs crystallized using 1500Å-thick a-Si spacer structure with channel length of 10 μm, in which the distance between neighboring a-Si spacers is 3 μm.

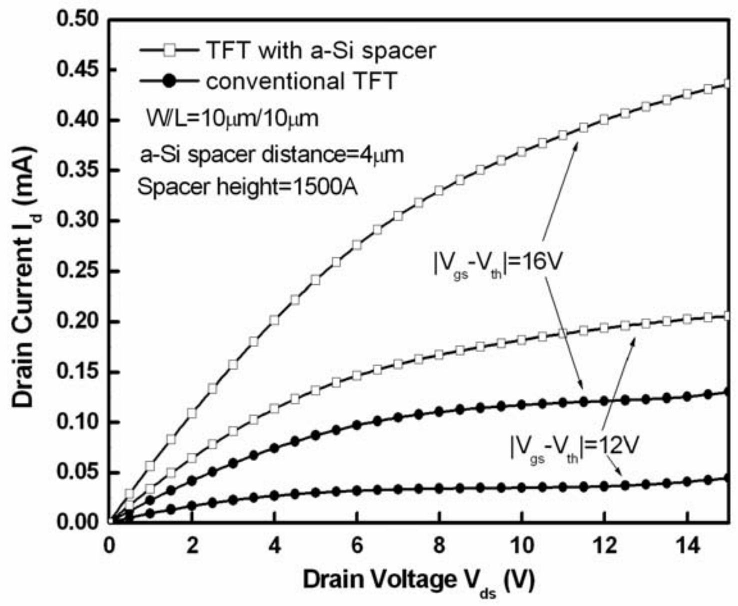

Figure 5.23(f). The output characteristics of ELC poly-Si TFTs crystallized using 1500Å-thick a-Si spacer structure with channel length of 10 μm, in which the distance between neighboring a-Si spacers is 4 μm.

As the device dimension is enlarged further, similar improvement in the electrical performance can also be observed. Figure 5.24(a) ~ Figure 5.24(e) and Figure 5.25(a) ~ Figure 5.25(b) compare the transfer and output characteristics of ELC poly-Si TFTs using a-Si spacer structure with those of conventional ones under different a-Si spacer design rules, respectively. The device channel length and width are both 20 μm. Table 5.4 summaries several important electrical characteristics of these devices. Very excellent-performance poly-Si TFTs with large device dimension are fabricated using this novel crystallization. Poly-Si TFTs with field effect mobility beyond 175 $cm^2$/V-s have been achieved in devices with spacer distance of 2.5 μm while the field effect mobility of the conventional ELC poly-Si counterparts is only about 100 $cm^2$/V-s. High on/off current ratio ($>10^7$) and low threshold voltage are also exhibited in these devices. The excellent performance of poly-Si TFT is ascribed to the high-quality poly-Si thin film in the device channel region.

**Table 5.4.** Measured optimal electrical characteristics of TFTs crystallized with conventional and a-Si spacer structure, in which the distances between neighboring a-Si spacers are 1 μm, 2 μm, 2.5 μm, 3 μm, and 4 μm, respectively.

| Structure (W=L=20μm) | Threshold Voltage (V) | Mobility ($cm^2/V\text{-}s$) | Subthreshold Swing (V/dec) | $I_{on}/I_{off}$ @ $V_{ds}$ = -5V |
|---|---|---|---|---|
| **Conventional TFT** | **5.97** | **104** | **1.53** | **$9.26\times10^{6}$** |
| **a-Si-spacer TFT<br>spacer distance = 1μm** | **5.56** | **129** | **1.55** | **$1.10\times10^{7}$** |
| **a-Si-spacer TFT<br>spacer distance = 2μm** | **4.99** | **162** | **1.49** | **$1.95\times10^{7}$** |
| **a-Si-spacer TFT<br>spacer distance = 2.5μm** | **4.59** | **176** | **1.53** | **$1.41\times10^{7}$** |
| **a-Si-spacer TFT<br>spacer distance = 3μm** | **4.75** | **158** | **1.47** | **$3.97\times10^{7}$** |
| **a-Si-spacer TFT<br>spacer distance = 4μm** | **5.11** | **151** | **1.49** | **$2.73\times10^{7}$** |

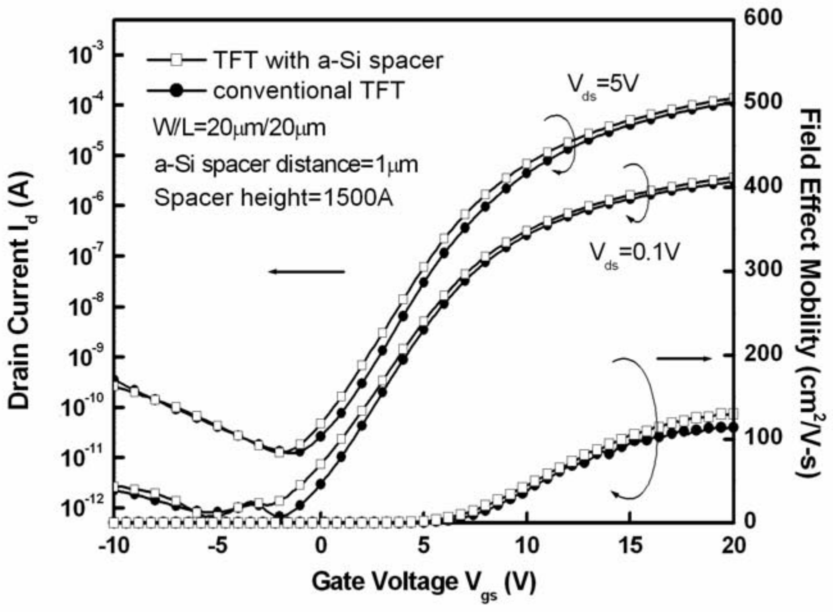

Figure 5.24(a). The typical transfer characteristics of poly-Si TFTs crystallized using 1500Å-thick a-Si spacer structure with channel length of 20 μm, in which the distance between neighboring a-Si spacers is 1 μm.

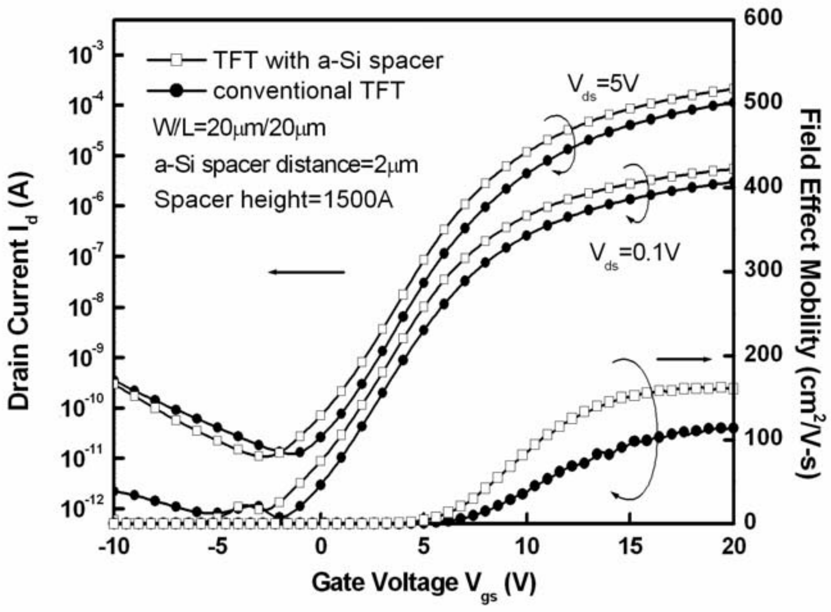

Figure 5.24(b). The typical transfer characteristics of poly-Si TFTs crystallized using 1500Å-thick a-Si spacer structure with channel length of 20 μm, in which the distance between neighboring a-Si spacers is 2 μm.

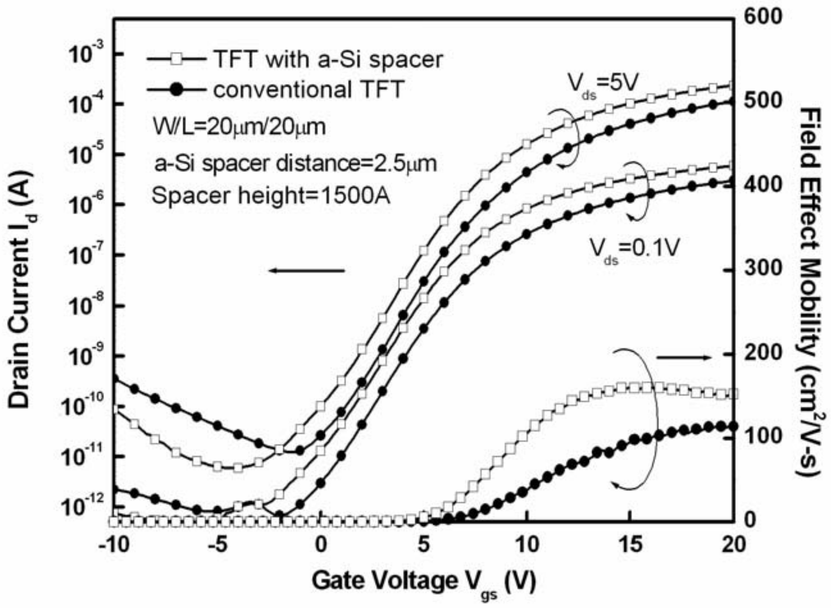

Figure 5.24(c). The typical transfer characteristics of poly-Si TFTs crystallized using 1500Å-thick a-Si spacer structure with channel length of 20 μm, in which the distance between neighboring a-Si spacers is 2.5 μm.

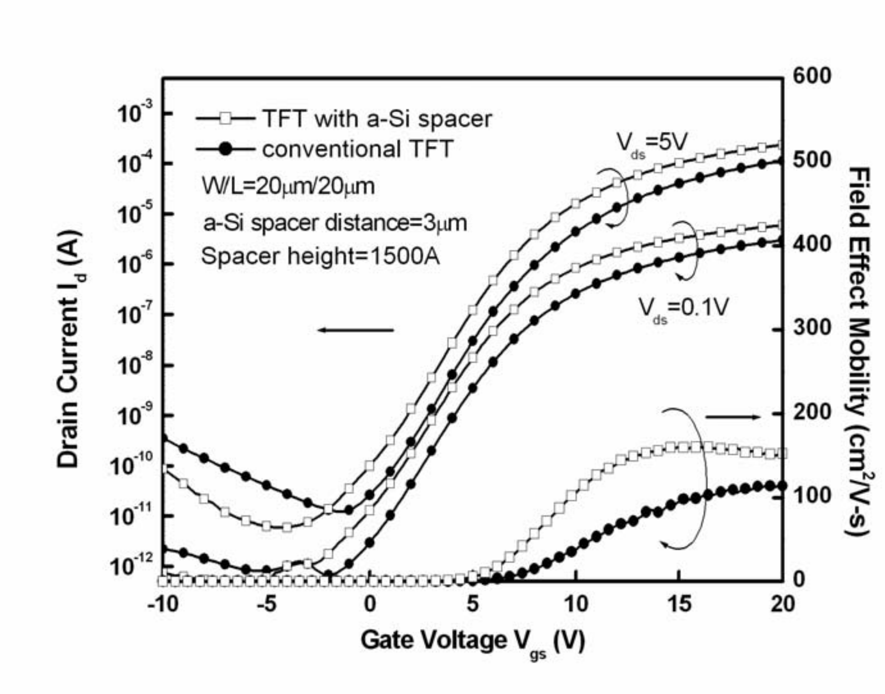

Figure 5.24(d). The typical transfer characteristics of poly-Si TFTs crystallized using 1500Å-thick a-Si spacer structure with channel length of 20 μm, in which the distance between neighboring a-Si spacers is 3 μm.

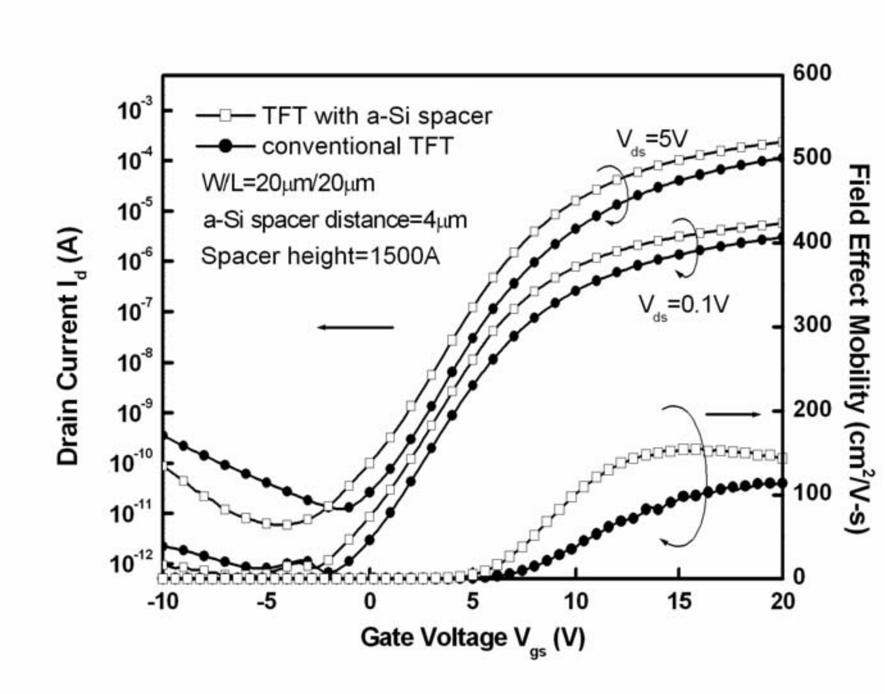

Figure 5.24(e). The typical transfer characteristics of poly-Si TFTs crystallized using 1500Å-thick a-Si spacer structure with channel length of 20 μm, in which the distance between neighboring a-Si spacers is 4 μm.

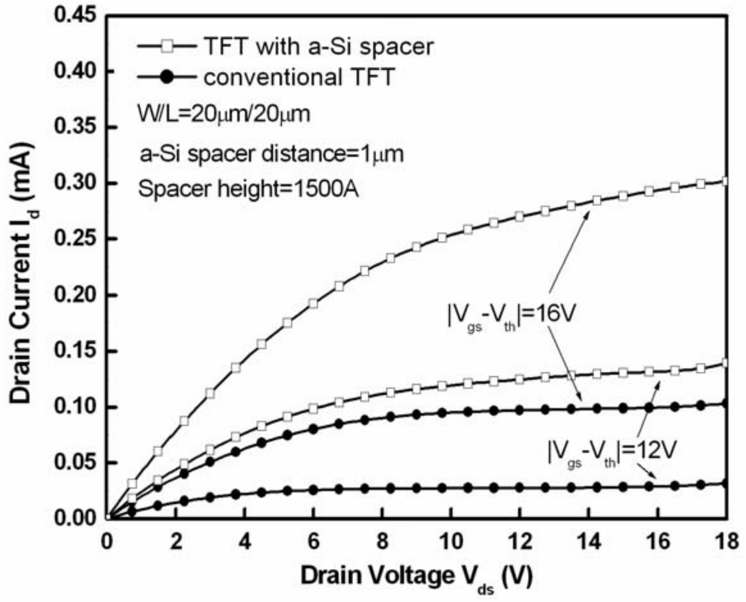

Figure 5.25(a). The output characteristics of poly-Si TFTs crystallized using 1500Å-thick a-Si spacer structure with channel length of 20 μm, in which the distance between neighboring a-Si spacers is 1 μm.

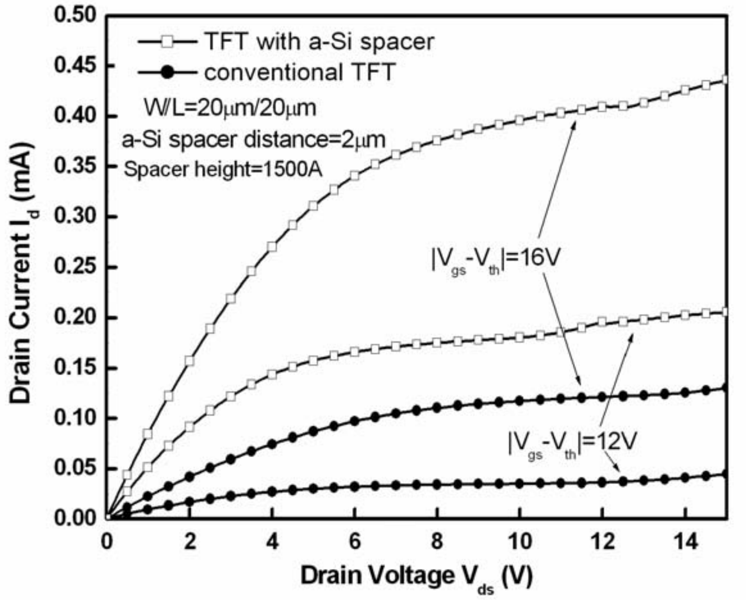

Figure 5.25(b). The output characteristics of poly-Si TFTs crystallized using 1500Å-thick a-Si spacer structure with channel length of 20 μm, in which the distance between neighboring a-Si spacers is 2 μm.

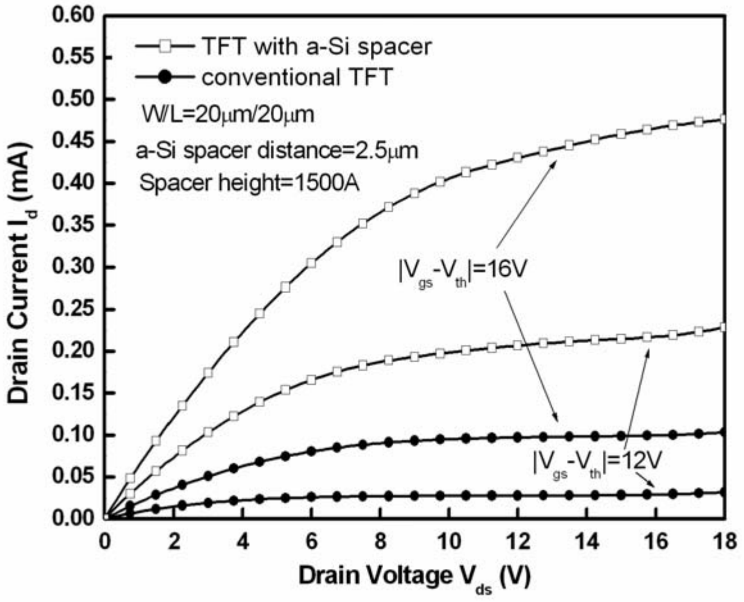

Figure 5.25(c). The output characteristics of poly-Si TFTs crystallized using 1500Å-thick a-Si spacer structure with channel length of 20 μm, in which the distance between neighboring a-Si spacers is 2.5 μm.

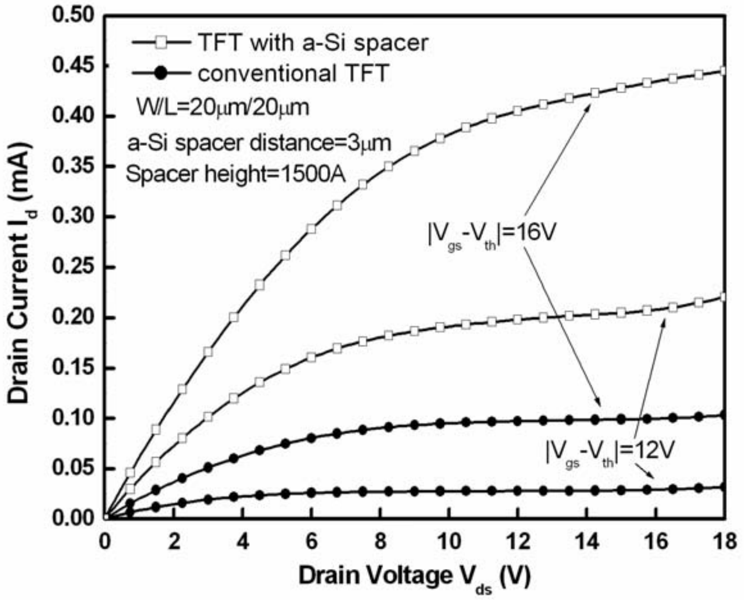

Figure 5.25(d). The output characteristics of poly-Si TFTs crystallized using 1500Å-thick a-Si spacer structure with channel length of 20 μm, in which the distance between neighboring a-Si spacers is 3 μm.

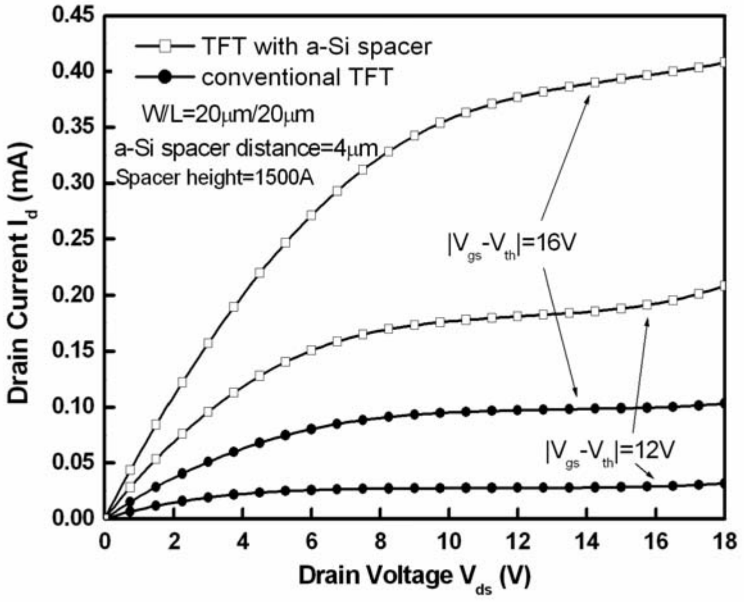

Figure 5.25(e). The output characteristics of poly-Si TFTs crystallized using 1500Å-thick a-Si spacer structure with channel length of 20 μm, in which the distance between neighboring a-Si spacers is 4 μm.

#### 5.4.3.2 a-Si Spacer with a Thickness of 2000Å

Figure 5.26(a) ~ Figure 5.26(f) show the typical transfer characteristics of poly-Si TFTs crystallized using 2000Å-thick a-Si spacer structure with channel length of 10 μm, in which the distances between neighboring a-Si spacers are 1 μm, 1.5 μm, 2 μm, 2.5 μm, 3 μm, and 4 μm, respectively. Several electrical characteristics are summarized in Table 5.5. Although fine and small grains are observed at the 2000Å-thick spacer region as discussed in the previous section, the poly-Si TFTs with a 2000Å-thick a-Si spacer still exhibit high field effect mobility than those of conventional counterparts. The largest field mobility is acquired as the distance between the neighboring a-Si spacers is 2.5 μm, which is consisting with the previous analysis results. However, due to the small grains existing in the channel region, the performance of the poly-Si TFTs with 2000Å-thick a-Si spacer structure is inferior to that of poly-Si TFTs with 1500Å-thick a-Si spacer structure.

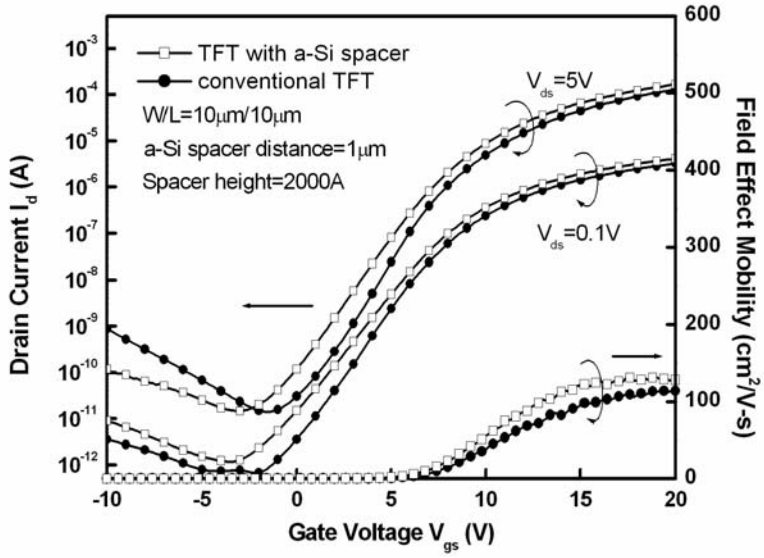

Figure 5.26(a). The typical transfer characteristics of poly-Si TFTs crystallized using 2000Å-thick a-Si spacer structure with channel length of 10 μm, in which the distances between neighboring a-Si spacer is 1 μm.

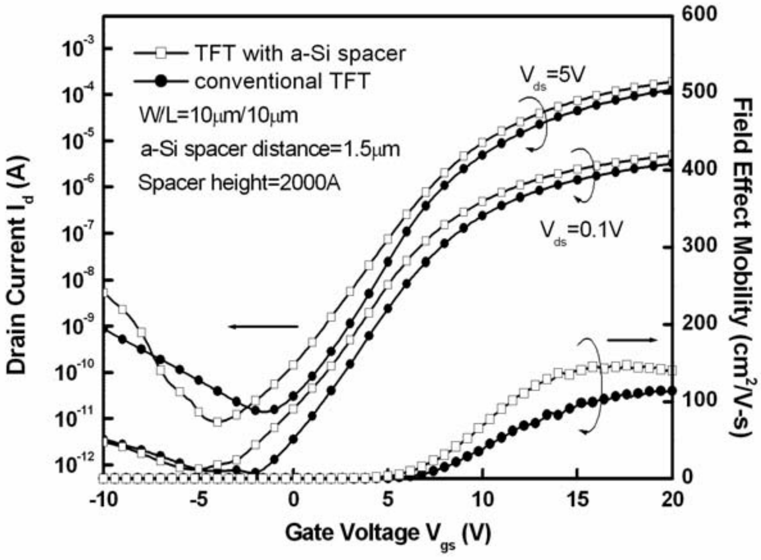

Figure 5.26(b). The typical transfer characteristics of poly-Si TFTs crystallized using 2000Å-thick a-Si spacer structure with channel length of 10 μm, in which the distance between neighboring a-Si spacers is 1.5 μm.

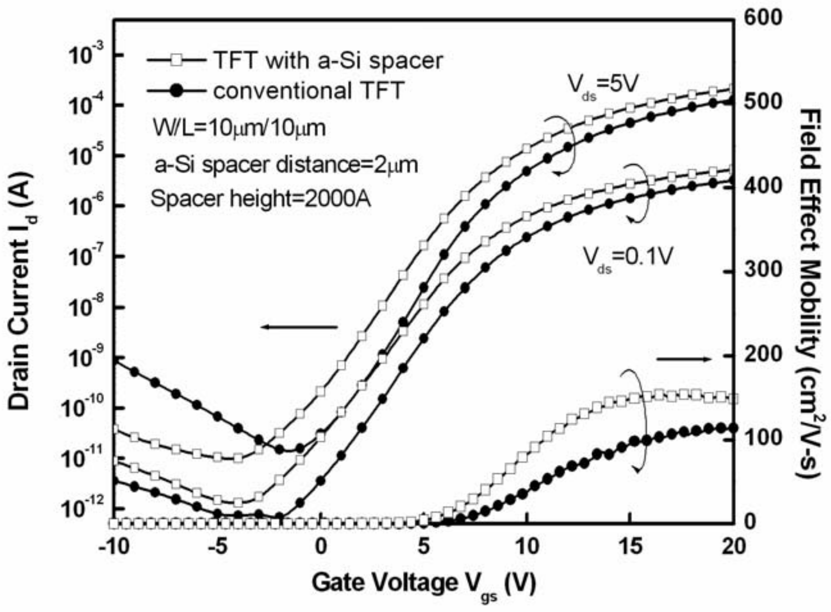

Figure 5.26(c). The typical transfer characteristics of poly-Si TFTs crystallized using 2000Å-thick a-Si spacer structure with channel length of 10 μm, in which the distance between neighboring a-Si spacers is 2 μm.

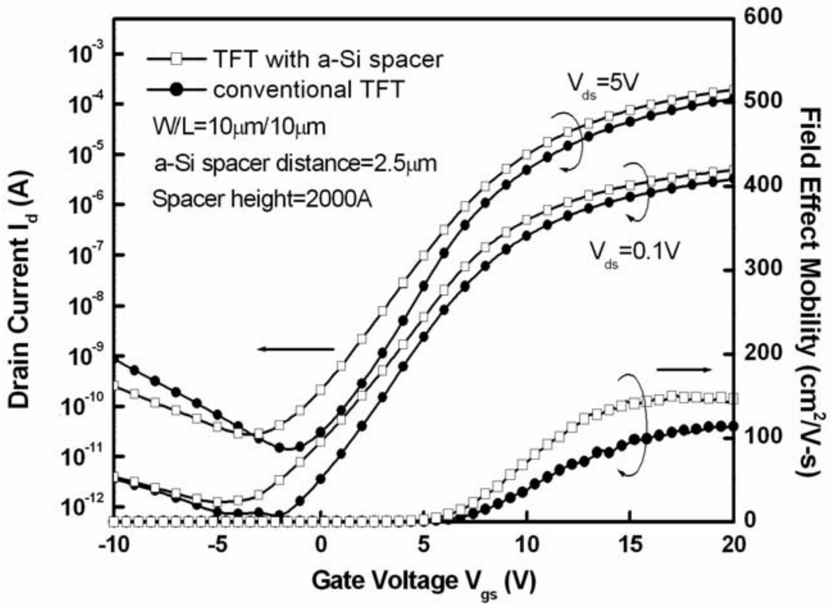

Figure 5.26(d). The typical transfer characteristics of poly-Si TFTs crystallized using 2000Å-thick a-Si spacer structure with channel length of 10 μm, in which the distance between neighboring a-Si spacers is 2.5 μm.

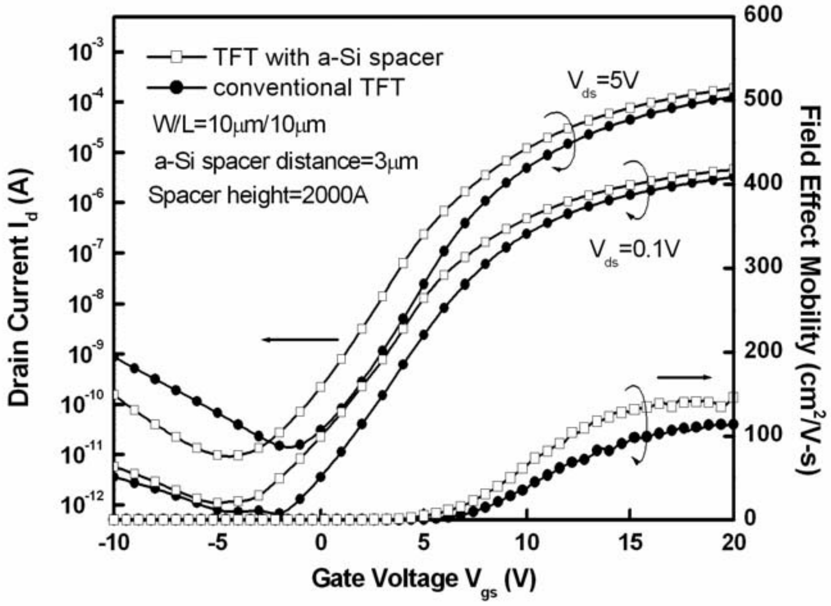

Figure 5.26(e). The typical transfer characteristics of poly-Si TFTs crystallized using 2000Å-thick a-Si spacer structure with channel length of 10 μm, in which the distance between neighboring a-Si spacers is 3 μm.

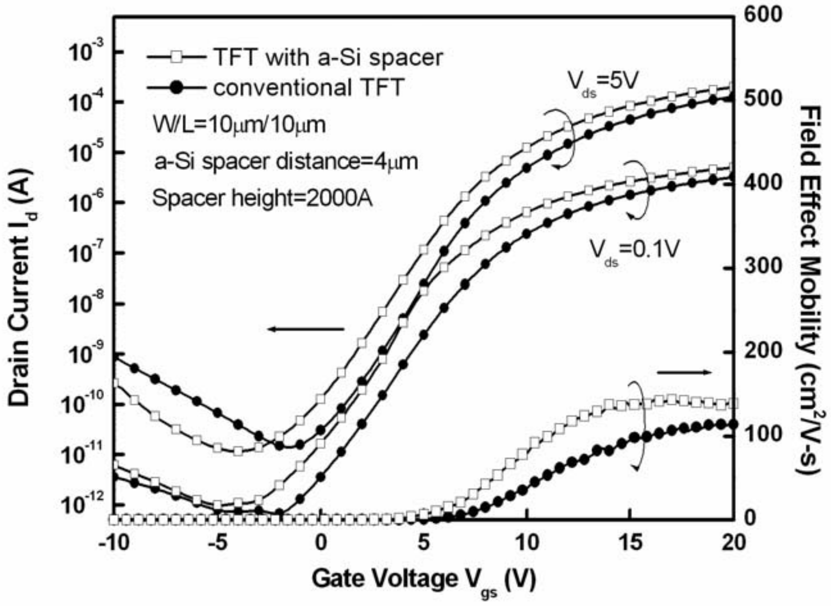

Figure 5.26(f). The typical transfer characteristics of poly-Si TFTs crystallized using 2000Å-thick a-Si spacer structure with channel length of 10 μm, in which the distance between neighboring a-Si spacers is 4 μm.

**Table 5.5**. Measured optimal electrical characteristics of TFTs crystallized with conventional and a-Si spacer structure, in which the distances between neighboring a-Si spacers are 1 μm, 1.5 μm, 2 μm, 2.5 μm, 3 μm, and 4 μm, respectively. The device channel length and width are 10μm. The a-Si spacer thickness is 2000Å.

| **Structure** | **Threshold Voltage (V)** | **Mobility ($cm^2$/V-s)** | **Subthreshold Swing (V/dec)** | **$I_{on}/I_{off}$ @ $V_{ds}$ = -5V** |
|---|---|---|---|---|
| **Conventional TFT** | **6.16** | **113** | **1.61** | **$9.27\times10^6$** |
| **a-Si-spacer TFT spacer distance = 1μm** | **5.53** | **135** | **1.78** | **$1.13\times10^7$** |
| **a-Si-spacer TFT spacer distance = 1.5μm** | **5.28** | **146** | **1.64** | **$2.24\times10^7$** |
| **a-Si-spacer TFT spacer distance = 2μm** | **5.03** | **151** | **1.70** | **$2.12\times10^7$** |
| **a-Si-spacer TFT spacer distance = 2.5μm** | **5.44** | **152** | **1.78** | **$6.99\times10^6$** |
| **a-Si-spacer TFT spacer distance = 3μm** | **4.40** | **145** | **1.58** | **$2.05\times10^7$** |
| **a-Si-spacer TFT spacer distance = 4μm** | **4.95** | **140** | **1.51** | **$1.72\times10^7$** |

Figure 5.27(a) ~ Figure 5.27(f) display the output characteristics of the ELC poly-Si TFTs crystallized using 2000Å-thick a-Si spacer structure with channel length of 10 μm. The distances between the adjacent a-Si spacers are 1 μm, 1.5 μm, 2 μm, 2.5 μm, 3 μm, and 4 μm, respectively. Similarly, high driving current can be found in these devices.

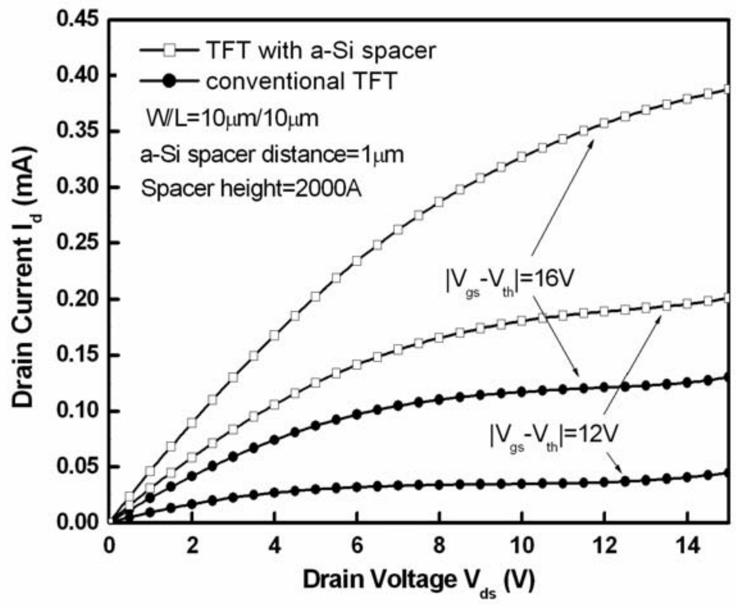

Figure 5.27(a). The output characteristics of poly-Si TFTs crystallized using 2000Å-thick a-Si spacer structure with channel length of 10 μm, in which the distance between neighboring a-Si spacers is 1 μm.

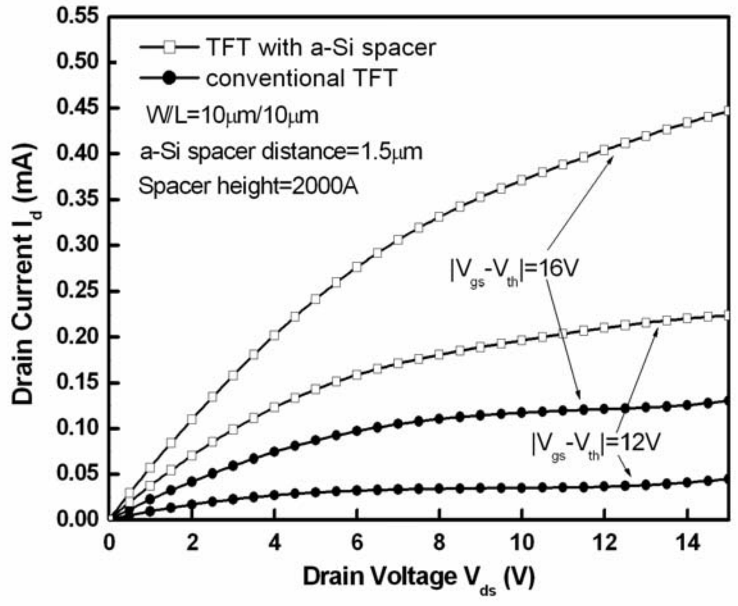

Figure 5.27(b). The output characteristics of poly-Si TFTs crystallized using 2000Å-thick a-Si spacer structure with channel length of 10 μm, in which the distance between neighboring a-Si spacers is 1.5 μm.

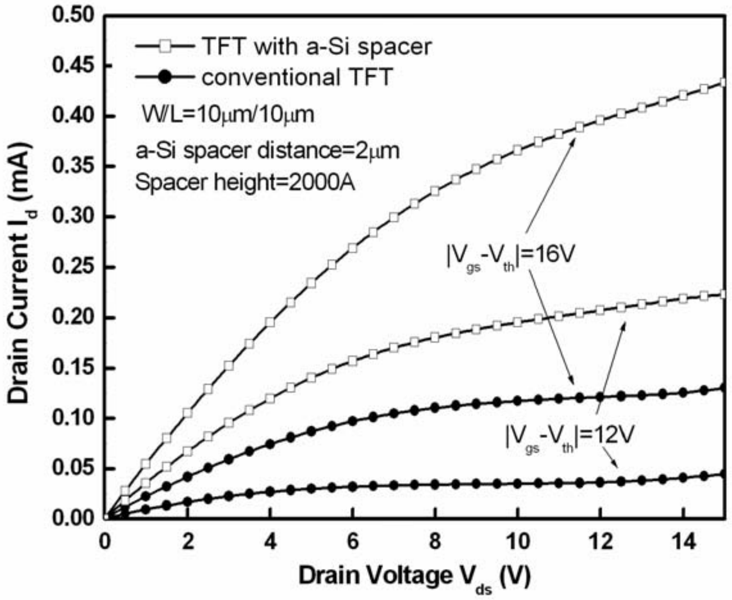

Figure 5.27(c). The output characteristics of poly-Si TFTs crystallized using 2000Å-thick a-Si spacer structure with channel length of 10 μm, in which the distance between neighboring a-Si spacers is 2 μm.

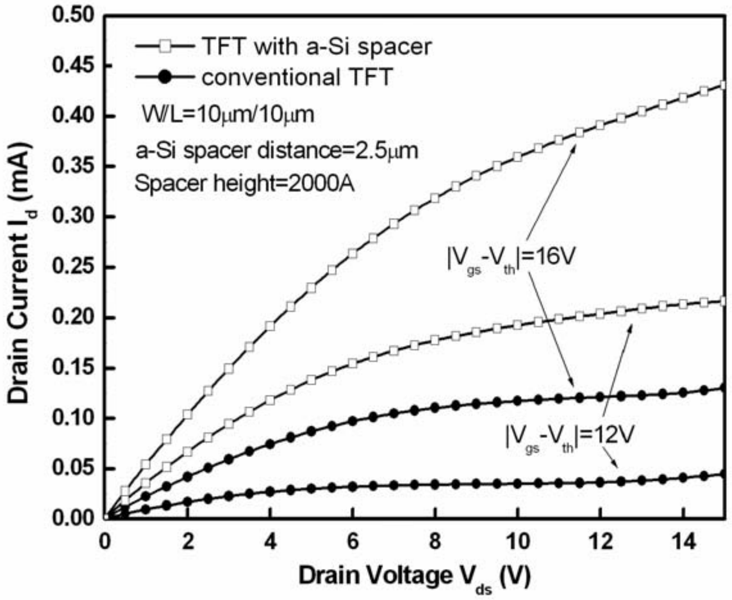

Figure 5.27(d). The output characteristics of poly-Si TFTs crystallized using 2000Å-thick a-Si spacer structure with channel length of 10 μm, in which the distance between neighboring a-Si spacers is 2.5 μm.

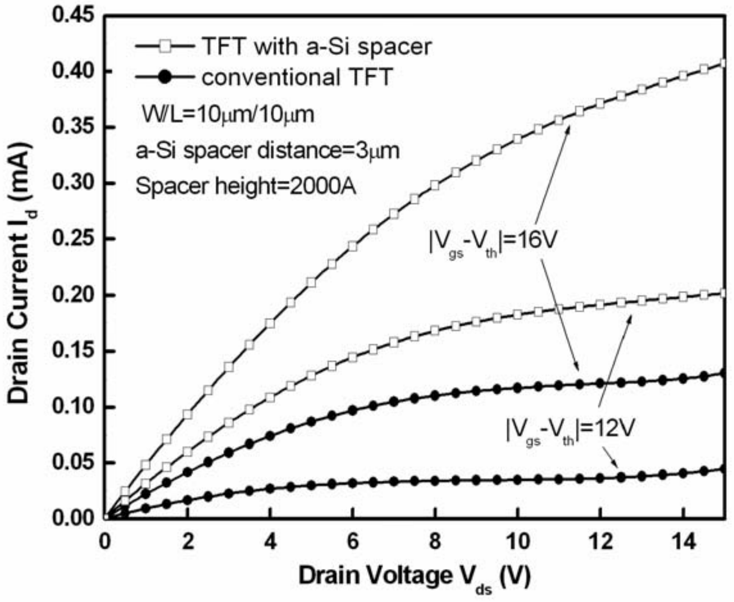

Figure 5.27(e). The output characteristics of poly-Si TFTs crystallized using 2000Å-thick a-Si spacer structure with channel length of 10 μm, in which the distance between neighboring a-Si spacers is 3 μm.

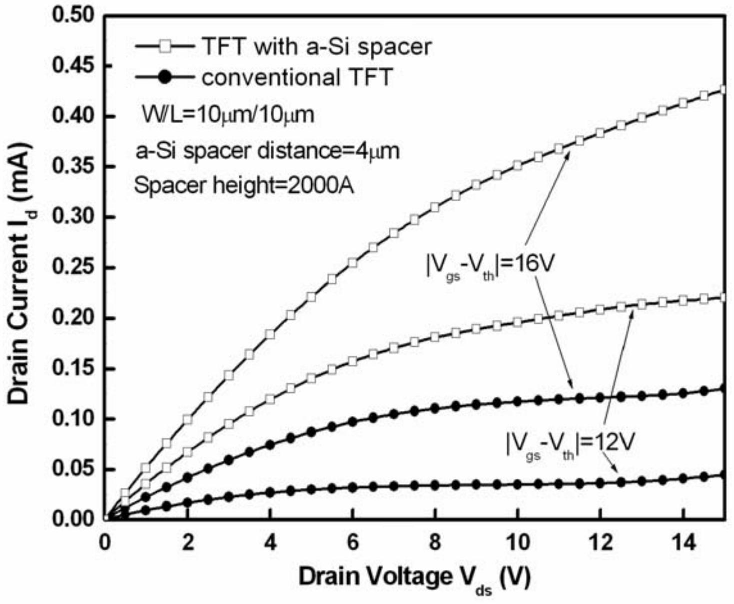

Figure 5.27(f). The output characteristics of poly-Si TFTs crystallized using 2000Å-thick a-Si spacer structure with channel length of 10 μm, in which the distance between neighboring a-Si spacers is 4 μm.

Figure 5.28(a) ~ Figure 5.28(e) and Figure 5.29(a) ~ Figure 5.29(e) compare the transfer and output characteristics of ELC poly-Si TFTs using a-Si spacer structure with those of conventional ones under W = L = 20 μm and different a-Si spacer design rules. The laser process conditions were optimized. Several electrical characteristics are summarized in Table 5.6. The poly-Si TFT fabricated by laser irradiation of a-Si spacer structure still exhibit better performance than those fabricated by conventional laser crystallization although a combination of small and the longitudinal grains are distributed in the channel region. Therefore, the a-Si spacer structure is suitable not only for small dimension TFT device but also for large dimension ones.

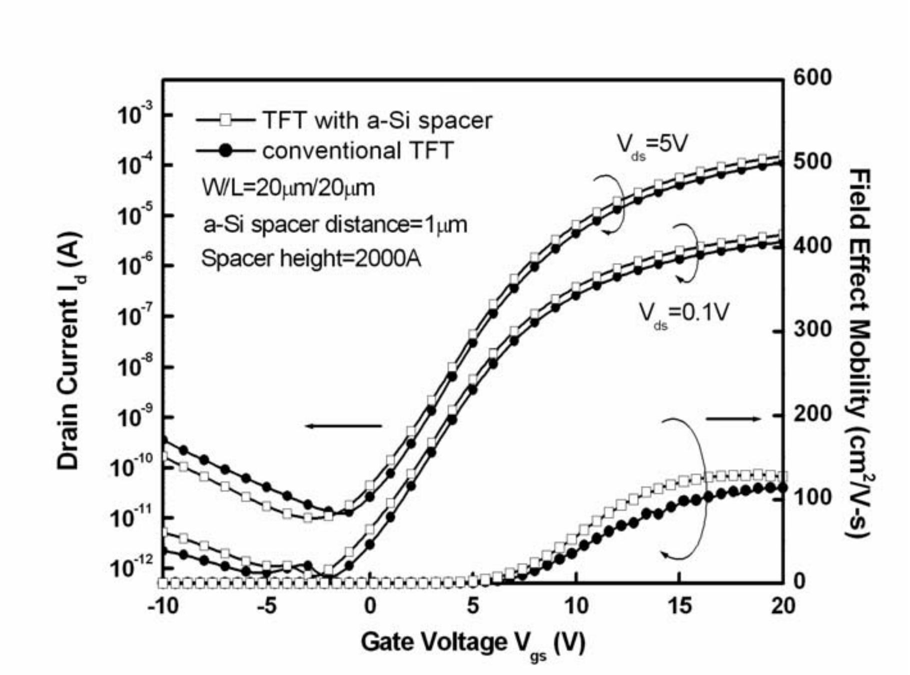

Figure 5.28(a). The typical transfer characteristics of poly-Si TFTs crystallized using 2000Å-thick a-Si spacer structure with channel length of 20 μm, in which the distance between neighboring a-Si spacers is 1 μm.

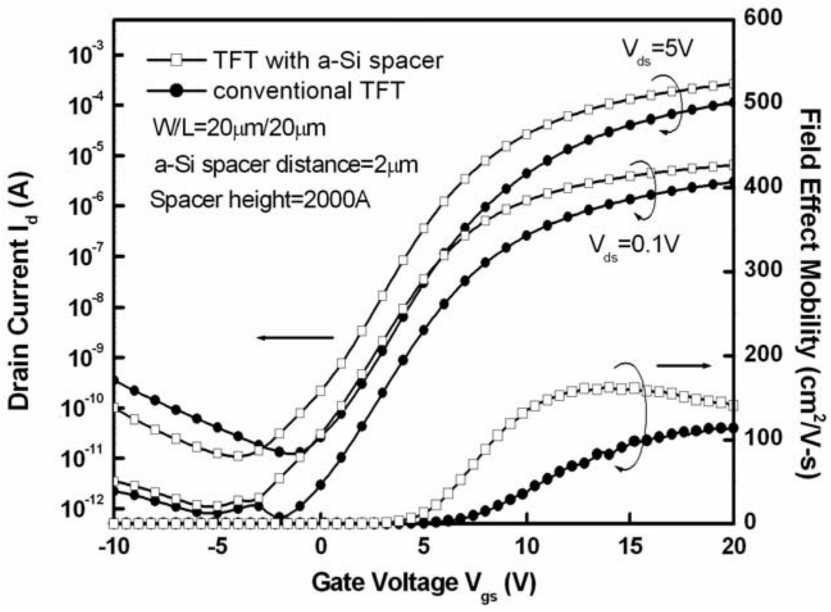

Figure 5.28(b). The typical transfer characteristics of poly-Si TFTs crystallized using 2000Å-thick a-Si spacer structure with channel length of 20 μm, in which the distance between neighboring a-Si spacers is 2 μm.

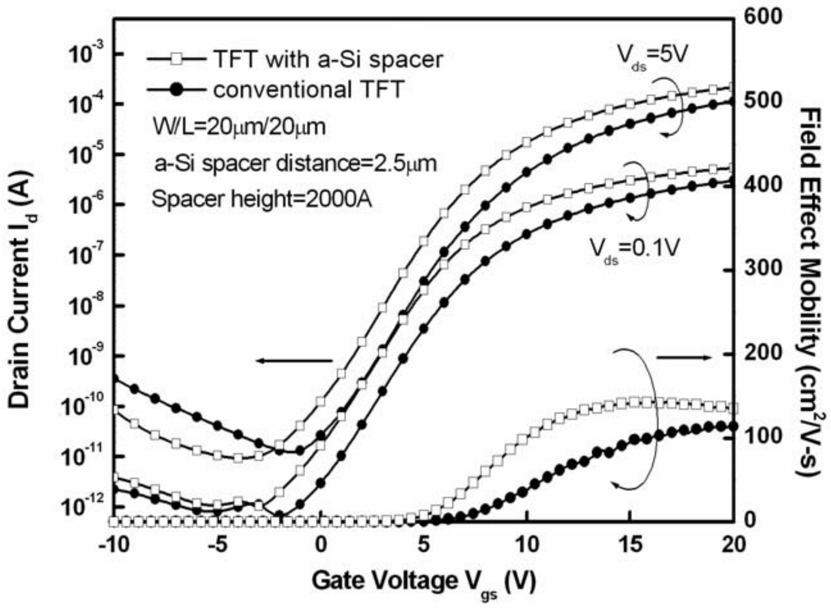

Figure 5.28(c). The typical transfer characteristics of poly-Si TFTs crystallized using 2000Å-thick a-Si spacer structure with channel length of 20 μm, in which the distance between neighboring a-Si spacers is 2.5 μm.

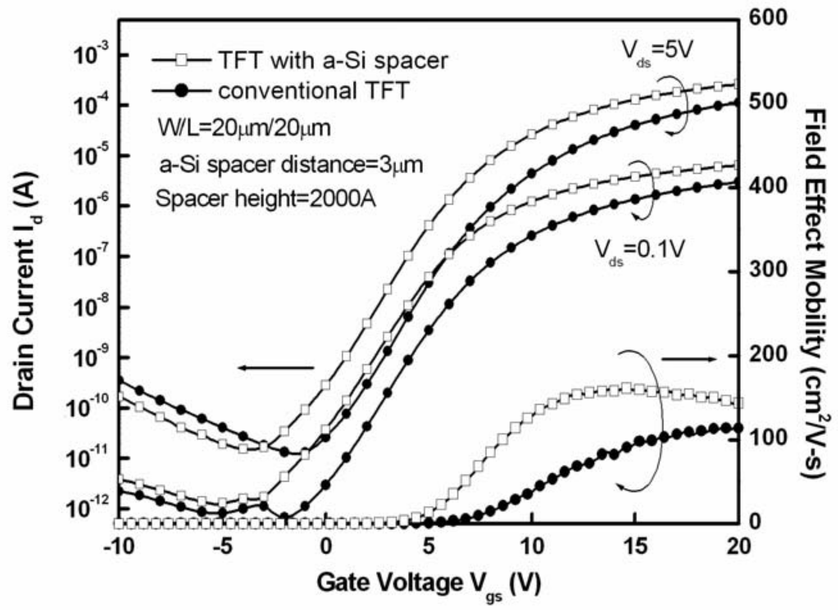

Figure 5.28(d). The typical transfer characteristics of poly-Si TFTs crystallized using 2000Å-thick a-Si spacer structure with channel length of 20 μm, in which the distance between neighboring a-Si spacers is 3 μm.

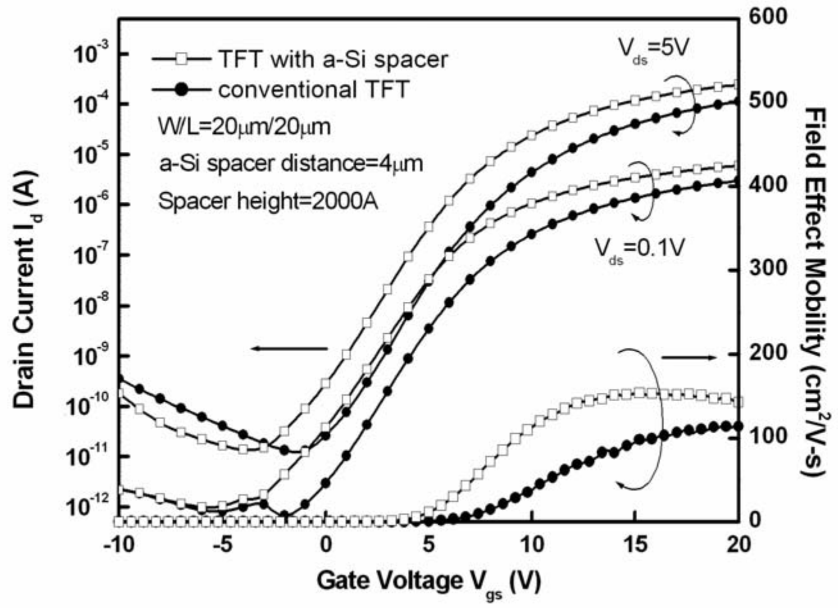

Figure 5.28(e). The typical transfer characteristics of poly-Si TFTs crystallized using 2000Å-thick a-Si spacer structure with channel length of 20 μm, in which the distance between neighboring a-Si spacers is 4 μm.

**Table 5.6**. Measured optimal electrical characteristics of TFTs crystallized with conventional and a-Si spacer structure, in which the distances between neighboring a-Si spacers are 1 μm, 2 μm, 2.5 μm, 3 μm, and 4 μm, respectively.

| Structure (W=L=20μm) | Threshold Voltage (V) | Mobility ($cm^2$/V-s) | Subthreshold Swing (V/dec) | $I_{on}/I_{off}$ @ $V_{ds}$ = -5V |
|---|---|---|---|---|
| **Conventional TFT** | **5.97** | **104** | **1.53** | **$9.26 \times 10^6$** |
| **a-Si-spacer TFT<br>spacer distance = 1μm** | **5.47** | **133** | **1.52** | **$1.55 \times 10^7$** |
| **a-Si-spacer TFT<br>spacer distance = 2μm** | **4.44** | **173** | **1.53** | **$2.41 \times 10^7$** |
| **a-Si-spacer TFT<br>spacer distance = 2.5μm** | **4.46** | **147** | **1.42** | **$2.32 \times 10^7$** |
| **a-Si-spacer TFT<br>spacer distance = 3μm** | **4.38** | **153** | **1.54** | **$1.77 \times 10^7$** |
| **a-Si-spacer TFT<br>spacer distance = 4μm** | **4.10** | **158** | **1.60** | **$1{,}79 \times 10^7$** |

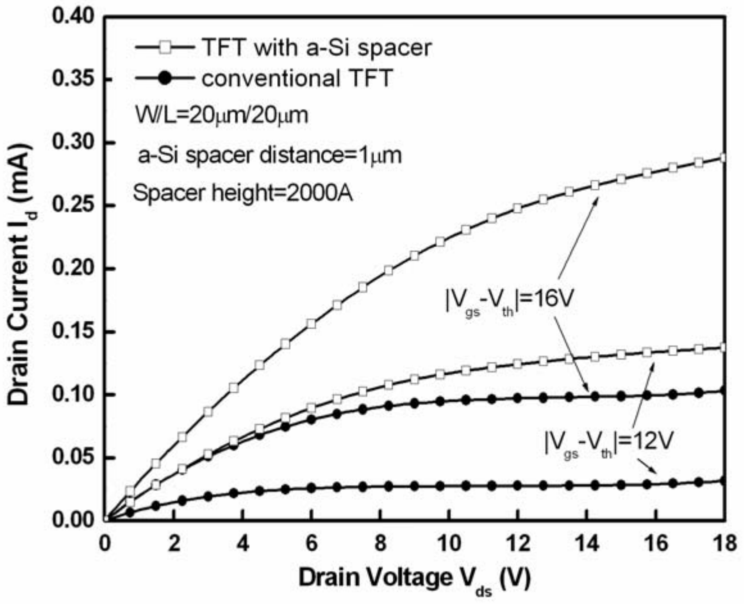

Figure 5.29(a). The output characteristics of poly-Si TFTs crystallized using 2000Å-thick a-Si spacer structure with channel length of 20 μm, in which the distance between neighboring a-Si spacers is 1 μm.

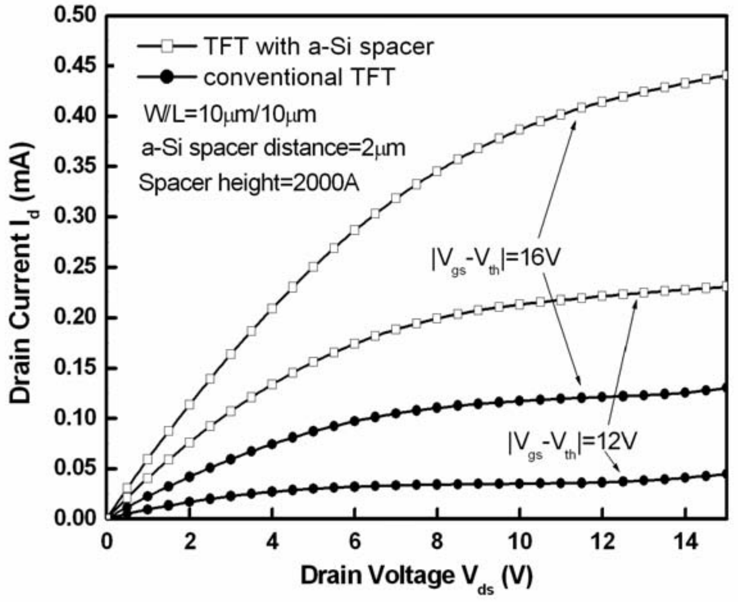

Figure 5.29(b). The output characteristics of poly-Si TFTs crystallized using 2000Å-thick a-Si spacer structure with channel length of 20 μm, in which the distance between neighboring a-Si spacers is 2 μm.

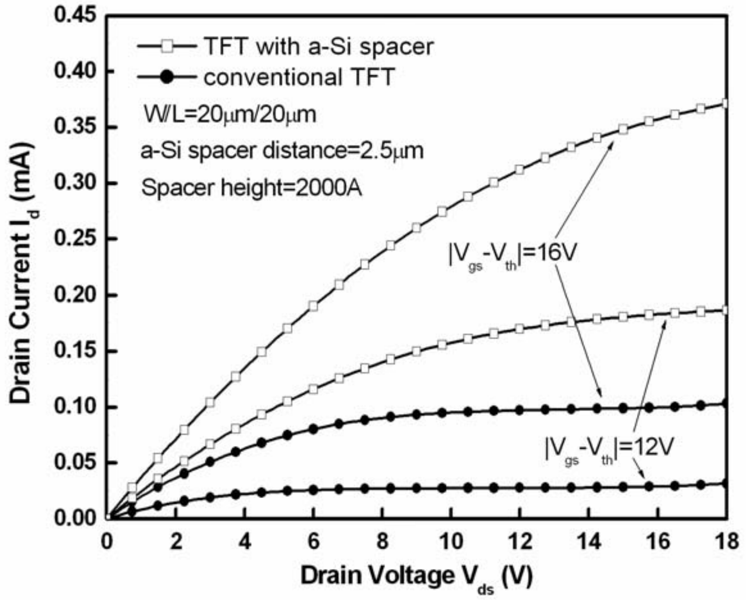

Figure 5.29(c). The output characteristics of poly-Si TFTs crystallized using 2000Å-thick a-Si spacer structure with channel length of 20 μm, in which the distance between neighboring a-Si spacers is 2.5 μm.

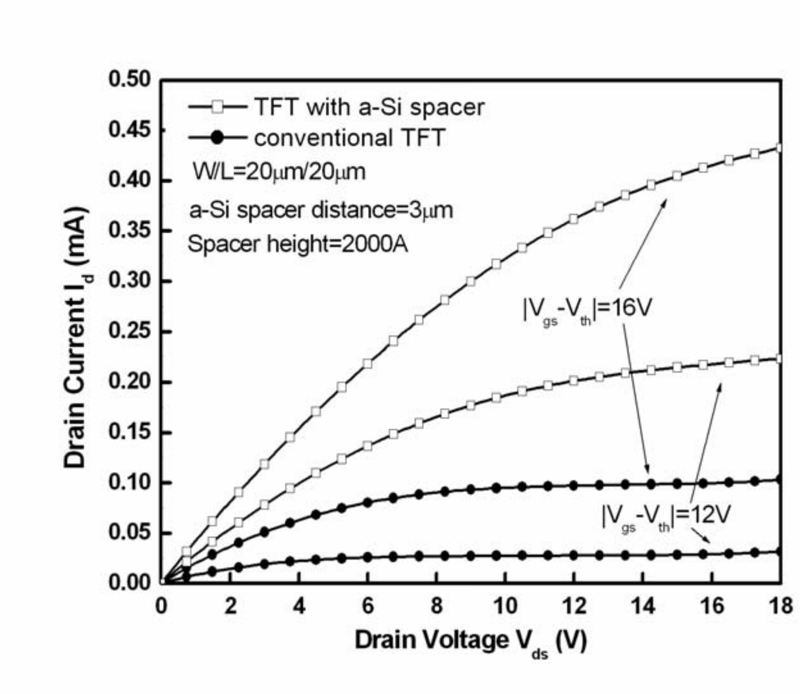

Figure 5.29(d). The output characteristics of poly-Si TFTs crystallized using 2000Å-thick a-Si spacer structure with channel length of 20 μm, in which the distance between neighboring a-Si spacers is 3 μm.

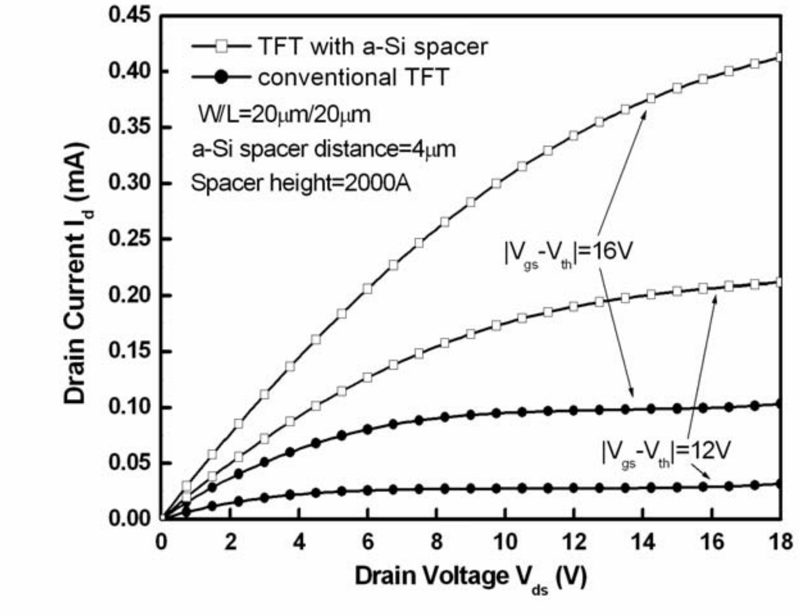

Figure 5.29(e). The output characteristics of poly-Si TFTs crystallized using 2000Å-thick a-Si spacer structure with channel length of 20 μm, in which the distance between neighboring a-Si spacers is 4 μm.

## 5.5 Summary

High-performance poly-Si TFTs with field-effect mobility exceeding 280 $cm^2/V$-s have been fabricated with a-Si spacer structure. The poly-Si TFTs with a-Si spacer structure exhibited better electrical characteristics than the conventional ones owing to the artificially controlled lateral grain growth. Large longitudinal grains were artificially grown measuring about 2.5 μm. Furthermore, the lateral growth starting from the a-Si spacer seed could progress along the opposite direction. Hence, when the channel region was designed to arrange at the spacer region, the grain boundaries perpendicular to the current flow in the channel region could be reduced. In addition to the enhancement of TFT performance, TFTs crystallized with a-Si spacer structure also demonstrated excellent uniformity due to the wide laser process window. This crystallization technique could be also applied to the large-dimension devices because periodic grain growth could be produced in the channel region. Better electrical performances were observed for the poly-Si TFTs crystallized with a-Si spacer structure under 10 μm and 20 μm design rules. Consequently, this spacer-seeded poly-Si TFTs could be considered for future system-on-panel applications because the circuits on a single panel needed varied sizes of TFT devices for different applications. .